DFPT Calculations on Phonons and Thermodynamic Properties in Mg-IV-N$_2$

Chaiyawat Kaewmeechai, Yongyut Laosiritaworn, and Atchara Punya Jaroenjittichai*

Abstract—**We investigated temperature dependent phonon and other associated properties of the Mg-IV-N$_2$ compounds, i.e high frequency (ε^∞) and static (ε^0) dielectric constants, Helmholtz free energy ($\triangle$F), internal energy ($\triangle$E), entropy ($\triangle$S), and specific heat capacity at constant volume (c$_v$). The phonons properties were calculated using the norm-conserving pseudopotential plane-wave method under the framework of density functional perturbation theory (DFPT) and local-density approximation (LDA). The results of the phonons show good agreement with the previous investigation on Mg-IV-N$_2$ and Zn-IV-N$_2$ compounds. In details, we found that the phonon frequency increases with increasing atomic number (Z) of group-IV as expected. In addition, the resulting of thermodynamic properties of MgSnN$_2$ is the first theoretical prediction and the result of MgSiN$_2$ is also consistent with experiments. Moreover, specific heat capacity of Mg-IV-N$_2$ compounds is approximately larger than that of the III-N by a factor of two, which implies higher capability in heat tolerance. However, dielectric constants of Mg-IV-N$_2$ are consistent to III-N, which reveal the similar response ability on electric field. From these results, Mg-IV-N$_2$ compounds infer themselves promising semiconductor candidates with thermal fluctuation sustainability for optoelectronic devices in the near future.**

Index Terms—**DFT, DFPT, Mg-IV-N$_2$ semiconductor, Phonon, Thermodynamic properties, Dielectric tensors.**

I. INTRODUCTION

THE III-nitride compounds are usually applied in the high-frequency optoelectronic devices, because of their wide band gap which has high performance for the light absorption and emission [1]. The thermal properties of these materials are also interesting due to the high thermal conductivity which implies that the heat can transfer very fast in the electronic devices [2]–[4]. Recently, alternative materials of III-nitride have been studied in both theory and experiment, especially II-IV-N$_2$ compounds. With the two different metal atoms on the cations, it is promising to be modified in the material design variously [5]. ZnSiN$_2$, ZnGeN$_2$, MgSiN$_2$, and MgGeN$_2$ compounds have been synthesised and found that their structure are in the space group of Pna2$_1$ (number 33) [6]–[9]. This structure can be expressed in the super-lattice wurtzite which is closely related to those of III-N semiconductors [10]. The electronic band

structures of these series have been investigated in theory by using density functional theory. It has been found that Zn-based and Mg-based IV-nitride with group IV-element (Si, Ge, and Sn) have related band gaps to the group of III-N especially the band gap of ZnGeN$_2$ and MgSiN$_2$ are similar to GaN and AlN respectively. It also has been found that the band gaps of ZnSiN$_2$ and MgSiN$_2$ are indirect while two other IV-based elements (Ge and Sn) are direct [5], [10]. The trends of the band gap of Mg-based and Zn-based IV-nitride are the same as the III-N compounds and usual semiconductors i.e. the band gap increases with the decrement of the lattice parameters. These theoretical studies also show excellent agreement with the experimental works [5], [10]–[12]. Not only electronic but also thermal properties of semiconductor devices have to be considered. The vibrational and related thermal properties of the ternary nitride are interested intensively. Thermodynamic properties and thermal expansion of MgSiN$_2$ were reported by fitting data from the experiments [8], [13], [14]. It shows that the specific heat capacity of MgSiN$_2$ is twice larger than AlN [13]. However, the experimental report of MgSiN$_2$ implies that the thermal conductivity (28 W m^{-1}kg^{-1}) is lower than that of AlN (200 W m^{-1}kg^{-1}) [14]. The phonons and related properties of Zn-IV-N$_2$ were estimated by using density functional perturbation theory. It can be seen that the trend of the related phonon properties depends on the group of IV: Si, Ge and Sn [15]. Recently, the vibrational properties of Mg-based IV-N$_2$ with substituting the group of IV by Si and Ge have been investigated [16], [17]. They reported phonon dispersion, Raman spectra, thermal properties, Born effective charge and high frequency dielectric tensors of MgSiN$_2$ and MgGeN$_2$ by using the projector augmented wave (PAW) method with the generalized gradient approximation of Perdew, Burke and Ernzerhof (PBE) [17]. For this work, we concentrate on the phonons and related properties of Mg-IV-N$_2$ compounds by using density functional theory. Although, there are the previous works which studied the vibrational and thermal properties of MgSiN$_2$ and MgGeN$_2$ [17], However, MgSnN$_2$ compound has not been synthesized and its phonon and thermal properties has not studied yet. To fulfill the understanding of Mg-IV-N$_2$ compounds, we expand to study phonons and related properties of MgSnN$_2$ and observe the trend of this series comparing to Zn-based IV-N$_2$ and III-N semiconductors.

II. COMPUTATIONAL DETAILS

Our calculation bases on density functional theory frame work by using norm-conserving pseudopotential method with local density approximation (LDA) for the exchange-correlation energy as implemented in ABINIT code [18]–[20]. The cutoff energy of the plane-wave was set to 80

TABLE I
LATTICE PARAMETERS (Å) OF Mg-IV-N_2

Compounds	LDA		
	a	b	c
MgSiN$_2$	6.4030[a]	5.2336[a]	4.9568[a]
MgGeN$_2$	6.5343	5.4182	5.1066
MgSnN$_2$	6.7131	5.7453	5.3124
Compounds	Experiment		
	a	b	c
MgSiN$_2$	6.4692[b]	5.2708[b]	4.9840[b]
MgGeN$_2$	6.611[c]	5.494[c]	5.166[c]

[a]Our previous LDA result of MgSiN2 from Ref. [23]
[b]Experimental result of MgSiN2 at 10 K from Ref. [8]
[c]Experimental result of MgGeN2 from Ref. [9]

TABLE II
BORN EFFECTIVE CHARGE TENSORS OF Mg-IV-N_2

MgSiN$_2$			
Atom	Z_{xx}	Z_{yy}	Z_{zz}
Mg	1.90	1.89	2.05
Si	3.04	3.19	3.14
N$_1$	2.48	-2.05	-3.03
N$_2$	-2.46	-3.03	-2.16
MgGeN$_2$			
Atom	Z_{xx}	Z_{yy}	Z_{zz}
Mg	1.91	1.84	2.00
Ge	3.01	3.20	3.17
N$_1$	-2.47	-2.07	-2.96
N$_2$	-2.44	-2.97	-2.20
MgSnN$_2$			
Atom	Z_{xx}	Z_{yy}	Z_{zz}
Mg	1.88	1.77	1.91
Sn	3.06	3.29	3.38
N$_1$	-2.46	-2.19	-2.94
N$_2$	-2.47	-2.86	-2.35

TABLE III
DIELECTRIC TENSORS OF Mg-IV-N_2

compounds	ε_{xx}^0	ε_{yy}^0	ε_{zz}^0	ε_{xx}^∞	ε_{yy}^∞	ε_{zz}^∞
MgSiN$_2$	4.20	4.27	4.33	7.85	8.48	9.79
MgGeN$_2$	4.58	4.73	4.72	8.18	8.89	9.70
MgSnN$_2$	5.06	5.22	5.28	8.40	8.87	9.89
Compounds	$\varepsilon_{\perp c}^0$		$\varepsilon_{\parallel c}^0$	$\varepsilon_{\perp c}^\infty$		$\varepsilon_{\parallel c}^\infty$
GaN[a]	5.25		5.41	9.22		10.32
AlN[b]	4.16		4.35	7.76		9.32

[a]Experimental result of GaN from Ref. [24]
[b]Experimental result of AlN from Ref. [25]

hartree and shifted 4×4×4 k-point grid was applied to the Brillouin zone integration. The equilibrium structure was optimized within the Hellmann-Feynman force tolerance of 10^{-6} hartree/Bohr. To generate phonon frequencies and related properties, the linear response approach within the density functional perturbation theory was performed [21]. The force constant and dielectric tensors will be obtained from the derivative of the energy. The longitudinal optical (LO) and transverse optical (TO) splitting at point was calculated corresponding to the long-range Coulomb forces character in polar compound by considering the Born effective charge tensors. The density of states and related thermal properties were estimated by considering the 20×20×20 q-point mesh by using the approach from Bungaro et al. [22].

III. RESULTS AND DISCUSSION

A. Crystal structure

The crystal structure of Mg-IV-N$_2$ compounds can be considered as ternary analogs to the IIIN materials. The cations of III-N are replaced with Mg and IV (Si, Ge and Sn) and the number of nitrogen atoms is doubled in order to complete the octet rule. The structure will be formed to be a superlattice of the wurtzite structure with 16 atoms per unit cell (four atoms for Mg and IV-element and eight atoms for N). This structure is categorized in the space group Pbn2$_1$ and in the point group of C$_{2v}$. The results of equilibrium structure as presented in table I imply that lattice parameters are in agreement with the experimental values within 2% deviation for MgSiN$_2$ and MgGeN$_2$. Whereas, the experimental study of the MgSnN$_2$ compound has not been reported yet. From the results, it can be seen that the lattice parameters calculated from LDA approximation underestimate the experimental results. On the other hand, the previous calculation using GGA approximation gives slightly higher values than those from experiments and LDA calculations [5], [17].

B. Dielectric and Born effective charge tensors

The high frequency dielectric tensors were calculated from the derivative of energy versus static electric field by the linear response approach. In the ionic compounds, the effect of long-range Coulomb force has to be considered to obtain LO-TO splitting of phonon frequency at Γ point by calculating the Born effective charge tensors and the nonanalytic term of the dynamics matrix [21]. The static dielectric tensors can be calculated using the result of Born effective charge in table II and the oscillator strength function. It can be seen that the trend of dielectric tensors increases when the group-IV are substituted with Si, Ge, and Sn respectively as seen in table III. This result can be observed from the previous work of Zn-IV-N$_2$ and III-N compounds [15], [24], [25]. In addition, we compare the dielectric constant of Mg-IV-N$_2$ with AlN and GaN. We found that the dielectric constants of AlN are between those of MgSiN$_2$ and MgGeN$_2$, while GaNs dielectric constants are close to those of MgSnN$_2$, which is a promising candidate material for terahertz devices in the future [24].

C. Phonon frequencies

The phonon modes can be classified with the irreducible representation of point group C$_{2v}$. We remark that A$_1$, B$_1$, and B$_2$ denote the modes in the vector along z, x, and y directions which correspond to the unit cell axes of c, a, and b respectively. A$_2$ mode is the rotational symmetry representation which does not respond to these three axes. From the 16 atoms in the unit cell, 48 phonon modes are obtained which can contribute 12 modes for each irreducible representation (A$_1$, A$_2$, B$_1$, and B$_2$). At the Γ point of Brillouin zone, the effect of the long-range Coulomb force was applied, and then the splitting between transverse and longitudinal modes will

TABLE IV
PHONON FREQUENCIES AT THE OF $MgGeN_2$

A_2	B_{1L}	B_{1T}	B_{2L}	B_{2T}	A_{1L}	A_{1T}
168.44	234.44	234.43	171.67	171.67	169.53	169.52
202.41	294.23	293.97	230.77	230.76	237.62	237.58
249.20	316.22	315.89	297.40	297.17	264.93	264.92
303.96	357.23	354.40	325.81	324.81	300.89	297.91
326.94	383.21	381.62	396.67	396.29	368.09	363.76
373.58	483.25	479.67	483.40	483.25	479.67	463.79
446.41	533.72	529.49	529.49	507.38	505.63	499.77
533.72	642.57	614.97	583.11	582.33	590.69	583.11
572.62	648.15	646.28	672.90	672.01	614.97	590.95
648.15	752.86	743.20	743.20	728.33	708.90	707.77
752.86	812.25	797.69	848.54	812.25	789.61	768.46
789.61						

TABLE V
PHONON FREQUENCIES AT THE OF $MgSnN_2$

A_2	B_{1L}	B_{1T}	B_{2L}	B_{2T}	A_{1L}	A_{1T}
128.65	181.46	181.15	122.13	122.12	118.47	118.46
138.32	209.49	209.11	176.88	176.88	183.85	183.81
225.98	306.98	306.81	269.03	268.12	234.30	234.20
252.36	332.10	331.88	306.81	306.43	276.36	275.77
307.75	360.73	360.68	369.93	369.91	346.54	345.41
354.85	488.14	485.82	489.78	489.39	485.82	475.30
471.58	519.61	514.44	514.44	503.91	503.91	501.27
519.61	606.24	582.72	580.13	568.33	568.33	557.62
555.29	617.79	610.46	621.58	617.79	582.72	580.13
606.24	678.51	677.69	677.69	677.56	662.18	662.18
678.51	756.44	724.24	723.05	717.17	717.17	679.15
723.05						

appear. When the static electric field was applied in the z, x, and y directions, the longitudinal corresponding modes (A_1, B_1, and B_2 modes) can be obtained. At the Γ point, the lowest phonon modes in z, x, and y directions (A_1, B_1, and B_2 modes) are all zero which are the phonon acoustic modes. So the remaining 78 modes are optical modes, we can classify 11 modes for each A_{1L}, A_{1T}, B_{1L}, B_{1T}, B_{2L} and B_{2T} mode. While the LO-TO splitting disappear in the A_2 mode, all 12 optical modes can be obtained only in this symmetry representation. The optical phonon frequencies in Mg-IV-N_2 are shown in the table IV and V. We notice that the trend of the phonon frequencies depends on group-IV in the Mg-IV-N_2. The highest phonon frequency is 1030.62 Ref. [23], 848.54, and 756.44 cm^{-1} in MgSiN$_2$, MgGeN$_2$, and MgSnN$_2$, respectively, which is also found in III-N and Zn-IV-N$_2$ [15], [26]. This is due to the increasing of atomic mass in group-IV element expands the lattice parameter and make atomic bond weaker. We compare the results with the previous work in MgSiN$_2$ and MgGeN$_2$ compound in the first-principle study [16], [17]. We found strongly agreement in the work with LDA, whereas the resulting with GGA gives slightly lower phonon frequencies. This can be explained by the difference between the structures (lattice parameters) obtained from LDA and GGA approximation. The phonon dispersions of Mg-IV-N_2 along the symmetry path in the Brillouin zone are presented in Fig. 1 and 2.We can observe 48 phonon branches from 16 atoms in a unit cell. At the Γ point, the discontinuity of the phonon branches due to LO-TO splitting can be observed. It can be seen that the phonon dispersion of Mg-IV-N_2 compounds are more complex than those of III-N [22], [26] which can cause the phonon-phonon scattering easier. This expectation can prove form the experiment in thermal conductivity at room temperature which found that the thermal conductivity of MgSiN$_2$ is considerably lower than that of AlN [14]. Therefore, we can predict that the heat can transfer fluently in the III-N than Mg-IV-N_2.

D. Thermodynamic properties

The thermodynamic properties of Mg-IV-N_2 i.e. Helmholtz free energy (ΔF), internal energy (ΔE), entropy (ΔS), and specific heat capacity at constant volume (C_v) were calculated from the phonon density of states with q-point of $20 \times 20 \times 20$ as presented in Fig.3,4 and 5. We
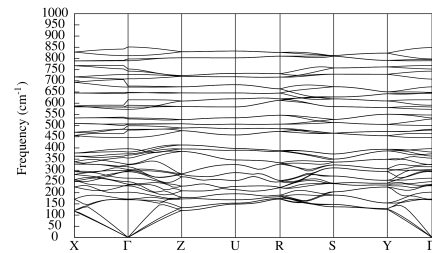

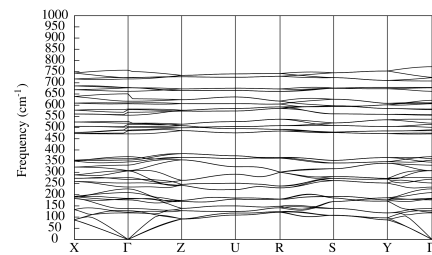Fig. 1. Phonon dispersions of MgGeN$_2$

Fig. 2. Phonon dispersions of MgSnN$_2$

can notice that the trend of all thermodynamic properties is related to the group IV-elements as same as phonon frequencies as shown in Fig. 6 and 7. This trend were also observed in the III-N and Zn-IV-N_2. Furthermore, we compare the results of C_v with the previous work of the experimental C_p of MgSiN$_2$, AlN and GaN using the assumption $C_p - C_v = 9V_m T\alpha^2/B_T$ where V_m, α, and B_T stand for the molar volume, linear expansion coefficient and isothermal compressibility [13]. We can use the experimental study in the thermal expansion of MgSiN$_2$ [8] to support the approximation of $C_p \sim C_v$ at the low temperature (below 300 K). Our result of C_v in MgGeN$_2$ and MgSnN$_2$ are clearly higher than experimental of C_p in MgSiN$_2$, AlN and GaN as seen in Fig. 8. We also compare the results of Mg-IV-N_2 with C_p the III-N in III$_2$-N$_2$ form, we found that the C_v of MgSiN$_2$ is strongly consistent with C_p of Al$_2$N$_2$ at low temperature below 300 K. In addition, we can observe the trend of C_p in GaN at low temperature is approximately equal to C_p of MgSnN$_2$.

IV. CONCLUSIONS

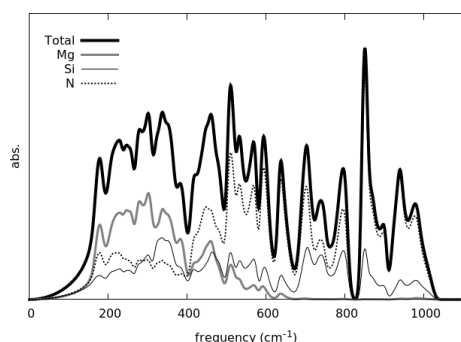The lattice vibration of Mg-IV-N_2 has been studied in the frame work of the density functional theory. The equilib-
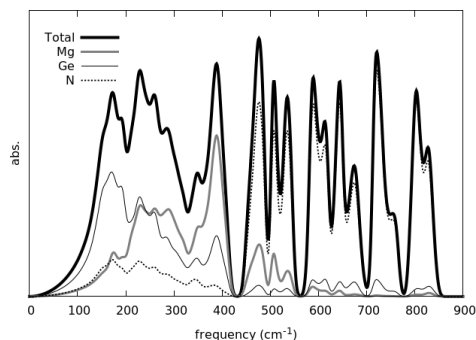
Fig. 3.   Phonon dispersions of MgSiN$_2$
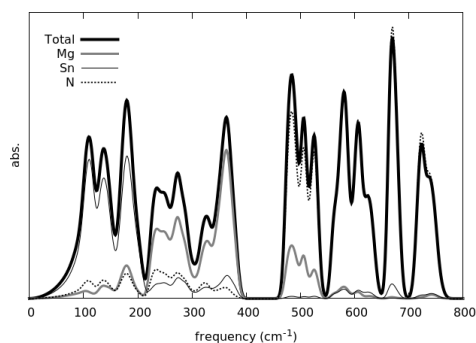

Fig. 4.   Phonon dispersions of MgGeN$_2$
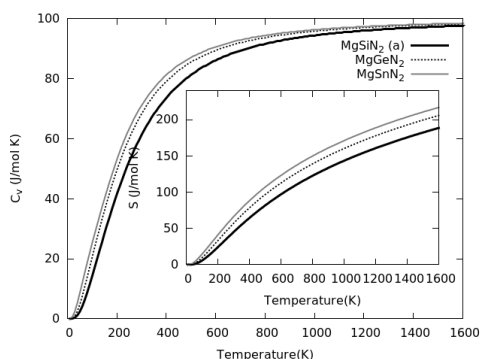

Fig. 5.   Phonon dispersions of MgSnN$_2$

Fig. 6.   Specific heat capacities at constant volume (C$_v$) and entropy (ΔS) of Mg-IV-N$_2$ as a function of temperature from 0-1600 K. , ^{a}Theoretical result of in MgSiN$_2$ from Ref. [23].

Fig. 7.   Helmholtz free energy (ΔF) and internal energy (ΔE) of Mg-IV-N$_2$ from 0-1600 K., ^{a}Theoretical result of in MgSiN$_2$ from Ref. [23].
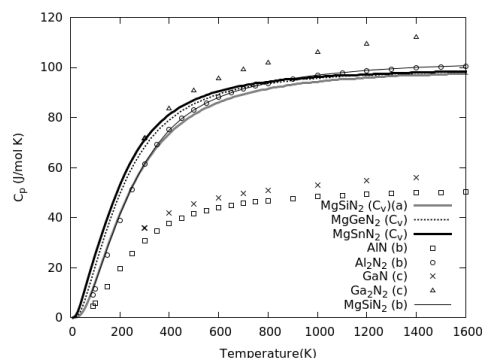
Fig. 8.   Fig. 5 Specific heat capacities at constant volume (C$_v$) of Mg-IV-N$_2$ comparing with available experiments of MgSiN$_2$, AlN and GaN., ^{a}Theoretical result of in MgSiN$_2$ from Ref. [23], ^{b}Experimental result of in AlN and MgSiN$_2$ from Ref. [14], ^{c}Experimental result of GaN from Ref. [27].

previous works in both theory and experiment. The LDA approximation gives slightly lower lattice constant than experiments with the relative different of 2%. The static and high frequency dielectric tensors of Mg-IV-N$_2$ are closely related to the AlN and GaN. In addition, the trends of phonon frequencies, dielectric tensors and thermodynamic properties depend on the group-IV element, similar to Zn-IV-N$_2$ and III-N semiconductors. The of Mg-IV-N$_2$ is strongly consistent to the experiment and it implies approximately two times larger than of AlN and GaN. The comparable properties of Mg-IV-N$_2$ to III-N promise a wider range of electronic device designs due to their structure with two cations.

rium structure, phonon frequencies, electric tensors, Born effective charge tensors and thermodynamic properties were calculated. The results are in good agreement with the
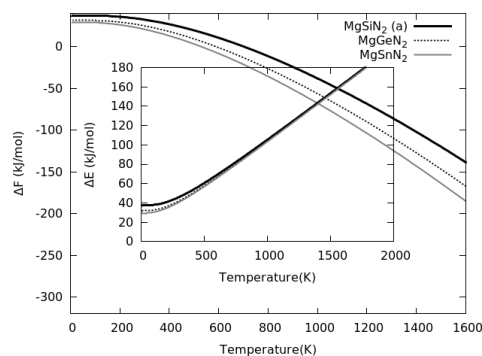
REFERENCES

[1] S. Strite and H. Morkoç, "Gan, Aln, and InN: A review," *Journal of Vacuum Science & Technology B: Microelectronics and Nanometer Structures Processing, Measurement, and Phenomena*, vol. 10, no. 4, pp. 1237–1266, 1992. [Online]. Available: https://avs.scitation.org/doi/abs/10.1116/1.585897

[2] A. AlShaikhi, S. Barman, and G. P. Srivastava, "Theory of the lattice thermal conductivity in bulk and films of GaN," *Phys. Rev. B*, vol. 81, p. 195320, May 2010. [Online]. Available: https://link.aps.org/doi/10.1103/PhysRevB.81.195320

[3] L. Lindsay, D. A. Broido, and T. L. Reinecke, "Thermal conductivity and large isotope effect in GaN from first principles," *Phys. Rev. Lett.*, vol. 109, p. 095901, Aug 2012. [Online]. Available: https://link.aps.org/doi/10.1103/PhysRevLett.109.095901

[4] A. AlShaikhi and G. P. Srivastava, "Thermal conductivity of single crystal and ceramic AlN," *Journal of Applied Physics*, vol. 103, no. 8, p. 083554, 2008. [Online]. Available: https://doi.org/10.1063/1.2908082

[5] A. P. Jaroenjittichai and W. R. Lambrecht, "Electronic band structure of Mg-IV-N_2 compounds in the quasiparticle-self-consistent GW approximation," *Physical Review B*, vol. 94, no. 12, p. 125201, 2016.

[6] A. Mintairov, J. Merz, A. Osinsky, V. Fuflyigin, and L. Zhu, "Infrared spectroscopy of $ZnSiN_2$ single-crystalline films on r-sapphire," *Applied Physics Letters*, vol. 76, no. 18, pp. 2517–2519, 2000.

[7] T. Misaki, A. Wakahara, H. Okada, and A. Yoshida, "Optical properties of $ZnGeN_2$ epitaxial layer," *physica status solidi (c)*, no. 7, pp. 2890–2893, 2003.

[8] R. Bruls, H. Hintzen, R. Metselaar, and C.-K. Loong, "Anisotropic thermal expansion of $MgSiN_2$ from 10 to 300 k as measured by neutron diffraction," *Journal of Physics and Chemistry of Solids*, vol. 61, no. 8, pp. 1285–1293, 2000.

[9] Y. David, J Laurent and J. Lang, "Structures of $MgSiN_2$ and $MgGeN_2$," *Bulletin de la Societe Francaise de Mineralogie et de Cristallographie*, vol. 93, no. 2, p. 153, 1970.

[10] A. Punya, W. Lambrecht, and M. Schilfgaarde, "Quasiparticle band structure of Zn-IV-N_2 compounds," vol. 84, p. 165204, 10 2011.

[11] J. B. Quirk, M. Råsander, C. M. McGilvery, R. Palgrave, and M. A. Moram, "Band gap and electronic structure of $MgSiN_2$," *Applied Physics Letters*, vol. 105, no. 11, p. 112108, 2014. [Online]. Available: https://aip.scitation.org/doi/abs/10.1063/1.4896134

[12] T. Boer, T. D. Boyko, C. Braun, W. Schnick, and A. Moewes, "Band gap and electronic structure of $MgSiN_2$ determined using soft X-ray spectroscopy and density functional theory," *physica status solidi (RRL)-Rapid Research Letters*, vol. 9, no. 4, pp. 250–254, 2015.

[13] R. J. Bruls, H. T. Hintzen, R. Metselaar, and J. Cees van Miltenburg, "Heat capacity of $MgSiN_2$ between 8 and 800 k," *The Journal of Physical Chemistry B*, vol. 102, no. 40, pp. 7871–7876, 1998.

[14] R. Bruls, H. Hintzen, and R. Metselaar, "A new estimation method for the intrinsic thermal conductivity of nonmetallic compounds: A case study for $MgSiN_2$, AlN and β-Si_3åN$_4$ ceramics," *Journal of the European Ceramic Society*, vol. 25, no. 6, pp. 767–779, 2005.

[15] T. R. Paudel and W. R. Lambrecht, "First-principles study of phonons and related ground-state properties and spectra in Zn-IV-N_2 compounds," *Physical Review B*, vol. 78, no. 11, p. 115204, 2008.

[16] S. Pramchu, A. P. Jaroenjittichai, and Y. Laosiritaworn, "Phonon and phonon-related properties of $MgSiN_2$ and $MgGeN_2$ ceramics: First principles studies," *Ceramics International*, vol. 43, pp. S444–S448, 2017.

[17] M. Råsander, J. Quirk, T. Wang, S. Mathew, R. Davies, R. Palgrave, and M. Moram, "Structure and lattice dynamics of the wide band gap semiconductors $MgSiN_2$ and $MgGeN_2$," *Journal of Applied Physics*, vol. 122, no. 8, p. 085705, 2017.

[18] J. P. Perdew and A. Zunger, "Self-interaction correction to density-functional approximations for many-electron systems," *Physical Review B*, vol. 23, no. 10, p. 5048, 1981.

[19] M. Fuchs and M. Scheffler, "Ab initio pseudopotentials for electronic structure calculations of poly-atomic systems using density-functional theory," *Computer Physics Communications*, vol. 119, no. 1, pp. 67–98, 1999.

[20] X. Gonze, F. Jollet, F. A. Araujo, D. Adams, B. Amadon, T. Applencourt, C. Audouze, J.-M. Beuken, J. Bieder, A. Bokhanchuk *et al.*, "Recent developments in the ABINIT software package," *Computer Physics Communications*, vol. 205, pp. 106–131, 2016.

[21] S. Baroni, P. Giannozzi, and E. Isaev, "Density-functional perturbation theory for quasi-harmonic calculations," *Reviews in Mineralogy and Geochemistry*, vol. 71, no. 1, pp. 39–57, 2010.

[22] C. Bungaro, K. Rapcewicz, and J. Bernholc, "Ab initio phonon dispersions of wurtzite AlN, GaN, and InN," *Physical Review B*, vol. 61, no. 10, p. 6720, 2000.

[23] C. Kaewmeechai, Y. Laosiritaworn, and A. P. Jaroenjittichai, "First-principles calculations of zone center phonons and related thermal properties of $MgSiN_2$," in *Journal of Physics: Conference Series*, vol. 901, no. 1. IOP Publishing, 2017, p. 012031.

[24] M. Hibberd, V. Frey, B. Spencer, P. Mitchell, P. Dawson, M. Kappers, R. Oliver, C. Humphreys, and D. Graham, "Dielectric response of wurtzite gallium nitride in the terahertz frequency range," *Solid State Communications*, vol. 247, pp. 68–71, 2016.

[25] W. Moore, J. Freitas Jr, R. Holm, O. Kovalenkov, and V. Dmitriev, "Infrared dielectric function of wurtzite aluminum nitride," *Applied Physics Letters*, vol. 86, no. 14, p. 141912, 2005.

[26] L.-C. Xu, R.-Z. Wang, X. Yang, and H. Yan, "Thermal expansions in wurtzite AlN, GaN, and InN: First-principle phonon calculations," *Journal of Applied Physics*, vol. 110, no. 4, p. 043528, 2011.

[27] J. Leitner, A. Strejc, D. Sedmidubskỳ, and K. Růžička, "High temperature enthalpy and heat capacity of GaN," *Thermochimica acta*, vol. 401, no. 2, pp. 169–173, 2003.